Electronic Supplementary Material (ESI) for Energy & Environmental Science.
This journal is © The Royal Society of Chemistry 2016

## Electronic Supplementary Information

# Au/Ag Core-shell Nanocuboids for High-efficiency Organic Solar Cells with Broadband Plasmonic Enhancement

Shenghua Liu,[a] Ruibin Jiang,[b] Peng You,[a] Xingzhong Zhu,[b] Jianfang Wang,[b] and Feng Yan*[a]

[a] *Department of Applied Physics, The Hong Kong Polytechnic University, Hung Hom, Kowloon, Hong Kong, China*
[b] *Department of Physics, The Chinese University of Hong Kong, Shatin, Hong Kong SAR, China.*

* Corresponding Author E-mail: apafyan@polyu.edu.hk

## Experimental Section

### Materials

Polythieno[3,4-b]-thiophene-benzodithiophene(PTB7), [6,6]-phenyl $C_{71}$-butyric acid methylester($PC_{71}BM$) and poly[4,8-bis(5-(2-ethylhexyl)thiophen-2-yl)-benzo[1,2-b;4,5-b'] dithiophene-2,6-diyl-alt-(4-(2-ethylhexyl)-3-fluorothieno[3,4-b]thiophene-)-2-carboxylate-2-6-diyl)] (PBDTTT-EFT) were purchased from 1-Materials Inc. The poly(3,4-ethylenedioxythiophene):polystyrene sulphonic acid (PEDOT:PSS) (Clevios™ P VP AI 4083) was purchased from Heraeus, Germany.

### Device fabrication

Au@Ag nanocuboid (NC) aqueous solutions ($2.27x10^{-10}$ M) with five different Ag shell thicknesses (5, 15, 20, 30 and 40 nm) were prepared by the method reported before.[37] The sizes of the Au cores in the experiment were kept identical. Five types of newly synthesized Au@Ag NC solutions were introduced into PEDOT:PSS aqueous solution with various volume ratios(1, 5, 10 and 20 vol. %). Then PEDOT:PSS hole transport layers of OPVs were prepared by coating the solutions on substrates. For conventional bulk heterojunction (BHJ) structure shown in Figure 1a, the pristine and Au@Ag introduced PEDOT:PSS were spin-coated onto the pre-cleaned ITO/glass substrates at 4000 rpm for 40 seconds (after $O_2$ plasma treatment for 6 min) and heated at 150°C for 1 h. While for the device structure of ITO/PEDOT:PSS/Au@Ag+active layer, Au@Ag NC ethanol solutions with the same concentration ($2.27x10^{-10}$ M) were spin-coated on the pristine PEDOT:PSS layer at the spin coating speed of 2000 rpm for 30 seconds, followed by 70˚C annealing for 5 mins. After that, the blend precursor of PTB7 and $PC_{71}BM$ (1:1.5 wt-ratio for 25 mg/ml) in the mixed solvents of chlorobenzene (CB) and 1,8-diiodoctane (DIO) (97%:3% in volume) was spin-cast on top of the PEDOT:PSS film at 1500 rpm for 1 min, followed by slow drying. Then, methanol was spin-coated onto the active layer at 2500 rpm for 60 seconds. Finally, a 20 nm-thick Ca layer and a 100 nm Al electrode were successively deposited on the active layer by thermal evaporation. The area of the active layer defined by the Al and ITO electrodes of the device

was 8.0 $mm^2$. All of the OPVs were then encapsulated in the glove box and tested in air.

Meanwhile, Au@Ag@$SiO_2$ NCs were also introduced into the PEDOT:PSS and the active layer. To eliminate the exciton quenching on the surface of the metal nanoparticles caused by direct contact between Au@Ag NCs and active layers, a ~10 nm-thick silica shell was synthesized to wrap up the Au(20 nm)@Ag(20 nm) NCs. The devices with the incorporation of Au@Ag@$SiO_2$ NCs into the PEDOT:PSS layer were fabricated at the optimized conditions (addition level: 5 vol.% NC aqueous solution with concentration of $2.27x10^{-10}$ M). For ITO/PEDOT:PSS/Au@Ag@$SiO_2$+active layer device, an Au@Ag@$SiO_2$ NC ethanol solution ($2.27x10^{-10}$M) was spin-cast at different rotations (1500, 2000, 2500, 3000 rpm) for 30s on top of PEDOT:PSS layers, then heated at 70˚C for 5 min. Both PTB7:$PC_{71}BM$ and PBDTTT-EFT:$PC_{71}BM$ were used as the active layer materials in our OPVs. All the preparation conditions of the OPVs based on PBDTTT-EFT:$PC_{71}BM$ were exactly the same as PTB7:$PC_{71}BM$ -based devices as described above.

**Material Characterization**

The absorption spectra of the aqueous solution containing Au/Ag NCs with different shell thicknesses as well as Au@Ag@$SiO_2$ NC ethanol solution were characterized by using a UV-VIS spectrophotometer (UV-2550, Shimadzu, Japan). Scanning electron microscopy (SEM, FEI Quanta 400 FEG microscope at 10 kV) was used to characterize the distribution of (20 nm)@Ag (20 nm) NCs on PEDOT:PSS film.

**Raman Characterization**

To explore the plasmonic effect of Au@Ag NCs embedded into the PEDOT:PSS layer, Raman spectroscopy was utilized to verify the enhanced plasmonic scattering effect in the Au (20 nm)@Ag (20 nm) NC -doped PEDOT:PSS thin film. Raman spectroscopy (HORIBA JOBIN YVON, HR800) with the excitation wavelength of 488 nm was used to extract Raman intensity on PEDOT:PSS layer incorporated by Au@Ag NCs. A 100× objective and around 1 mm laser spot was used to focus the laser beam and collect the Raman signal.

The Raman characterization was carried out on a sample with the structure of glass/ITO/PEDOT:PSS+Au@Ag at the optimized addition level (5 vol.%). Pristine PEDOT:PSS thin film without NCs was also characterized as a reference. As depicted in Figure S3a, the Raman intensity was significantly improved when 5 vol.% Au (20 nm)@Ag(20 nm) NCs were incorporated into the PEDOT:PSS layer (red curve) compared to the pristine one (black curve). Specifically, the highest Raman shift peak around 1448 $cm^{-1}$ increased from 218.8 of the pristine PEDOT:PSS film to 452.5 after Au@Ag incorporation. Over 100% enhancement of the Raman intensity suggests that the LSPR of the Au (20 nm)@Ag(20 nm) NCs could dramatically improve the light absorption of the film.

**TEM Characterization**

The transmission electron microscopy (TEM) images of Au@Ag NCs with different shell thicknesses (5, 15, 20 nm) were observed under a TEM (2100F, Japan).

The PEDOT:PSS thin film incorporated with Au@Ag NCs as well as the NC distribution embedded into the PEDOT layer were observed under the TEM. A ~40 nm-thick PEDOT:PSS thin film incorporated with 5 vol.% Au (20 nm)@Ag (20 nm) NCs was spin-cast onto a Cu foil. After thermal annealing at 150°C for 1 h, the sample was placed in an aqueous solution of ferric nitrate at room temperature. In terms of the high solubility of PEDOT:PSS in $H_2O$, before spin-coating, a 3 vol.% cross linker, 3-glycidoxypropyltrimethoxysilane ($C_9H_{20}O_5Si$) was added into the PEDOT:PSS precursor as a cross linker to solidify the PEDOT:PSS polymer networks after annealing treatment. After 2 hours' etching in $Fe(NO_3)_3$ solution, an uniform NC incorporated PEDOT:PSS layer was obtained when the Cu foil underneath was completely dissolved away. As shown in Figure S3b, the semi-transparent PEDOT:PSS thin film with Au(20 nm)@Ag (20 nm) NCs ( addition level: 5 vol.%) was floated on the surface of $Fe(NO_3)_3$ solution. The inset image depicted the PEDOT:PSS layers coated on Cu foils before etching. The film was then transferred into deionized (DI) water. Finally, a micro copper grid for TEM was placed in the DI water to load the floating PEDOT:PSS thin film. The PEDOT:PSS film was taken out of water and dried for several hours before TEM characterization. We can clearly find that the distribution of Au@Ag NCs is relatively uniform in the PEDOT:PSS layer without particle aggregation. Approximately 4.5 NCs were contained in 1 $(\mu m)^2$ PEDOT:PSS layer as indicated in Figure S3c.

**Simulation**

FDTD simulation was performed by using the software FDTD Solutions 7.5 developed by Lumerical Solutions, Inc. During the simulations, an electromagnetic pulse in the wavelength range from 300 to 1000 nm was launched into a box containing a target nanostructure. A mesh size of 0.5 nm was employed in calculating the electric field enhancements of the Au@Ag and Au@Ag@$SiO_2$ NCs. The dielectric function of gold and silver were taken from previously measured values [P. B. Johnson, R. W. Christy, Phys. Rev. B 1972, 6, 4370-4379. E. D. Palik, Handbook of Optical constants of solids, vol.1 Academic Press, Orlando, USA 1985]. The refractive index (n) of PEDOT:PSS and $SiO_2$ medium were assumed to be 1.45 and 1.4, respectively,[41] while PTB7:$PC_{71}BM$ medium was calculate to have an average refractive index of 1.8 at the wavelength region of 500-650 nm.[42] The sizes of the nanostructures were determined according to the average sizes measured from the TEM images.

**Figures**:

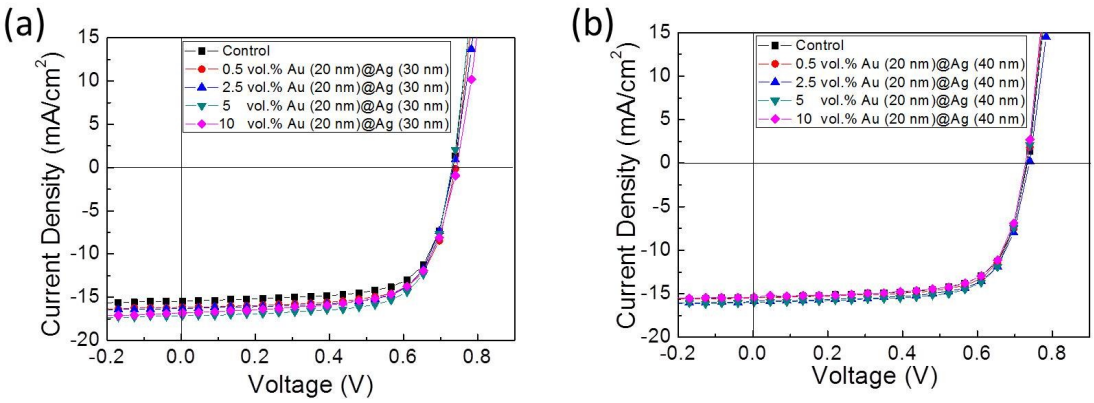


**Figure S1.** Current density-voltage (J-V) curves of the best control device and the OPVs with various addition levels (0.5, 2.5, 5, 10 vol%) of (a) Au(20nm)@Ag(30nm), (b) Au(20nm)@Ag(40nm) NCs.

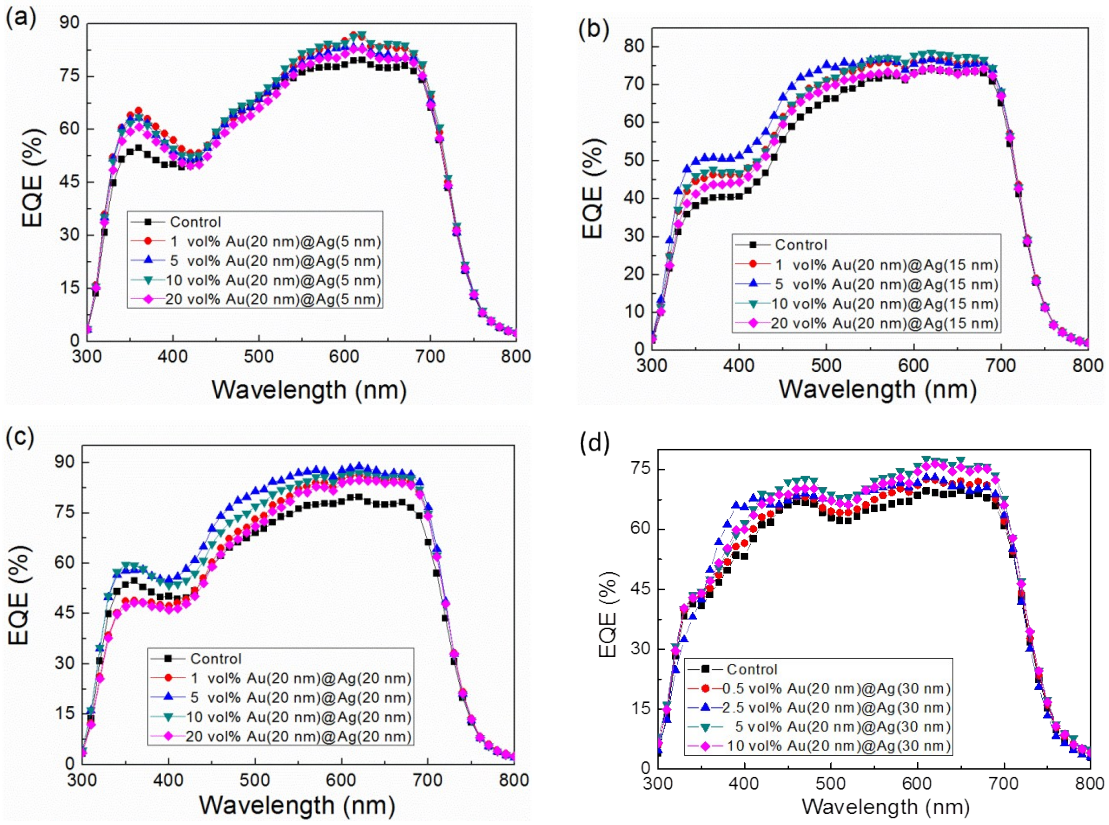

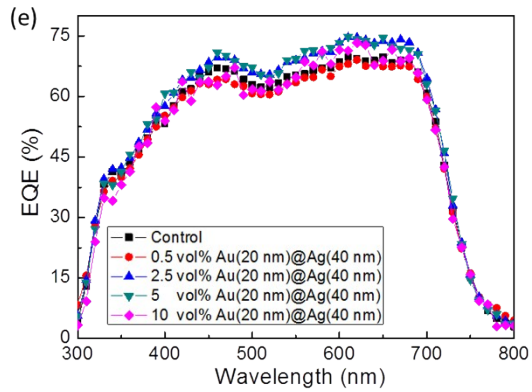


**Figure S2.** EQE spectra of the OPVs based on PTB7:$PC_{71}BM$ with the incorporation of various Au@Ag NCs in PEDOT:PSS layers of different additions levels. (a) Au (20 nm)@Ag (5 nm) with the Ag shell thickness of 5nm; (b) Au (20 nm)@Ag(15 nm) with the Ag shell thickness of 15 nm; (c) Au (20 nm)@Ag (20 nm) with the Ag shell thickness of 20 nm; (d) Au (20 nm)@Ag (30 nm) with the Ag shell thickness of 30 nm; (e) Au (20 nm)@Ag (40 nm) with the Ag shell thickness of 40 nm.

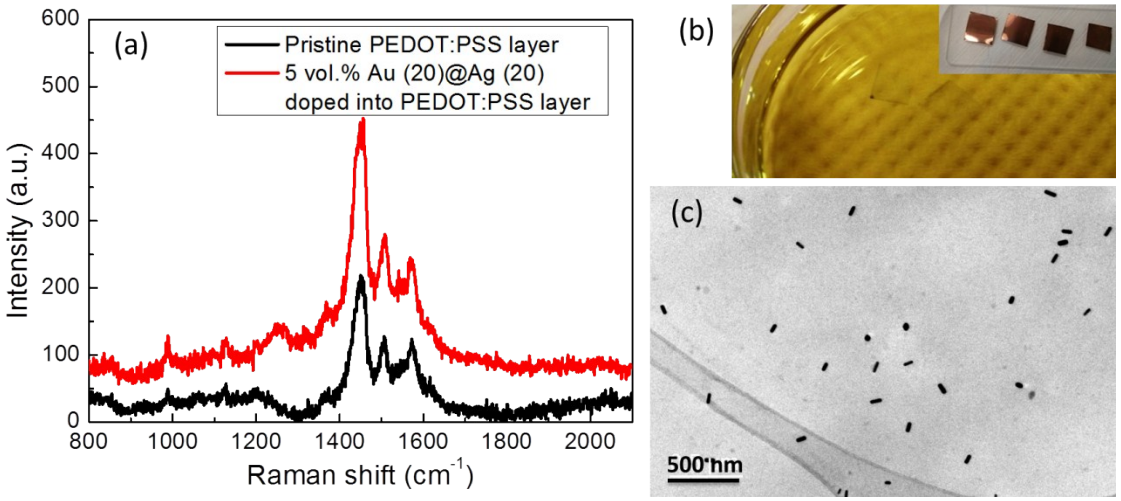


**Figure S3**. (a) Raman intensity of a pristine PEDOT:PSS layer (black curve) and a PEDOT:PSS film incorporated with 5 vol.% Au (20 nm)@Ag (20 nm) NCs (red curve). The samples were excited by a 488 nm laser. (b) An uniform thin film of PEDOT:PSS floated on the surface of $Fe(NO_3)_3$ solution after etching the Cu substrate. (c) TEM image of PEDOT:PSS thin film with the incorporation of Au (20 nm)@Ag (20 nm) NCs.

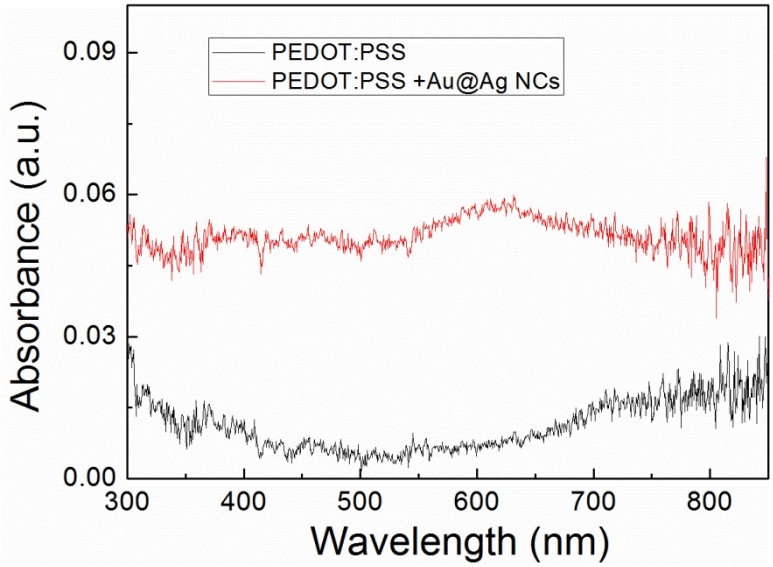


**Figure S4**. Light absorbance of a pure PEDOT:PSS film and a PEDOT:PSS film with the incorporation of Au(20 nm)@Ag(20 nm) NCs.

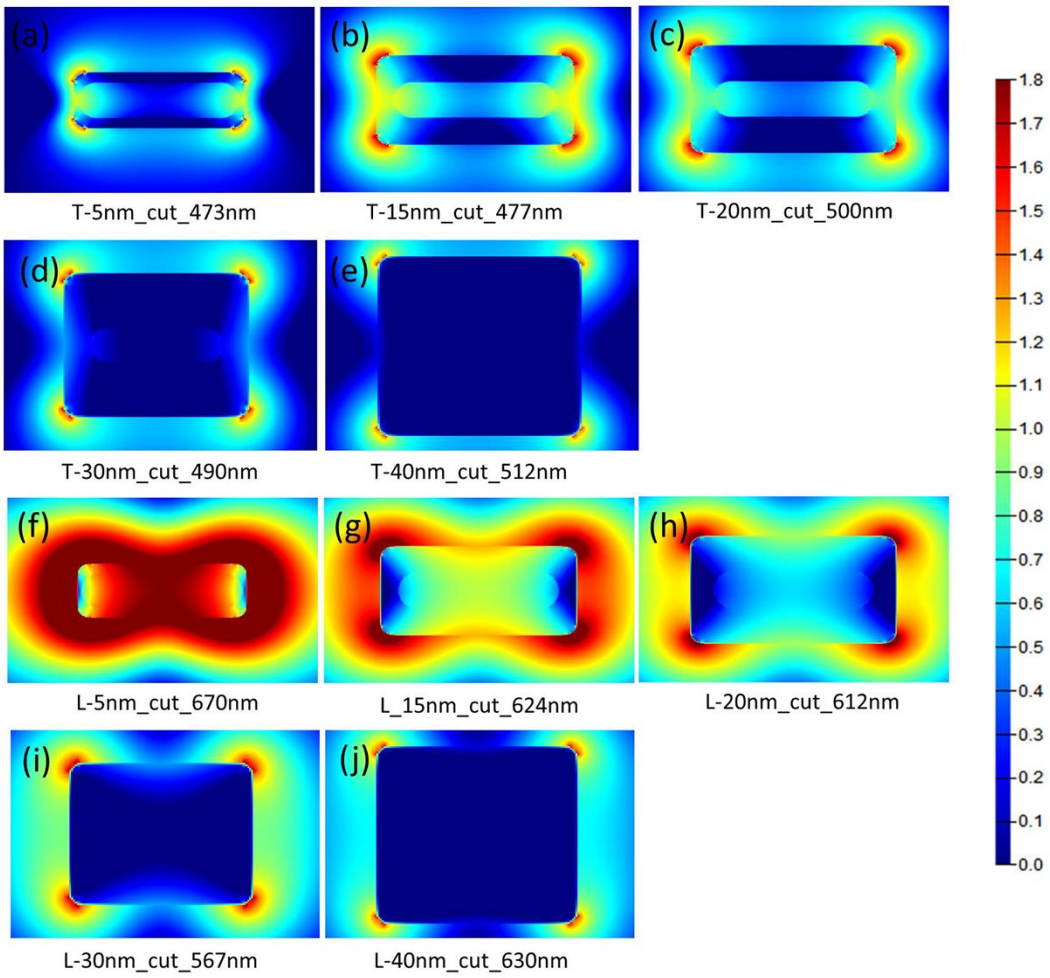


**Figure S5**. Electric field distribution at corresponding resonance wavelengths for Au@Ag NCs with different Ag shell thicknesses (5, 15, 20, 30, 40 nm) in PEDOT:PSS medium simulated by FDTD method. (a, b, c, d, e) are for transverse dipole mode and (f, g, h, i, j) for longitudinal dipole mode, respectively with the resonance wavelengths indicated in the figures. The enhancement of the electric field intensity is presented at the logarithmic scale.

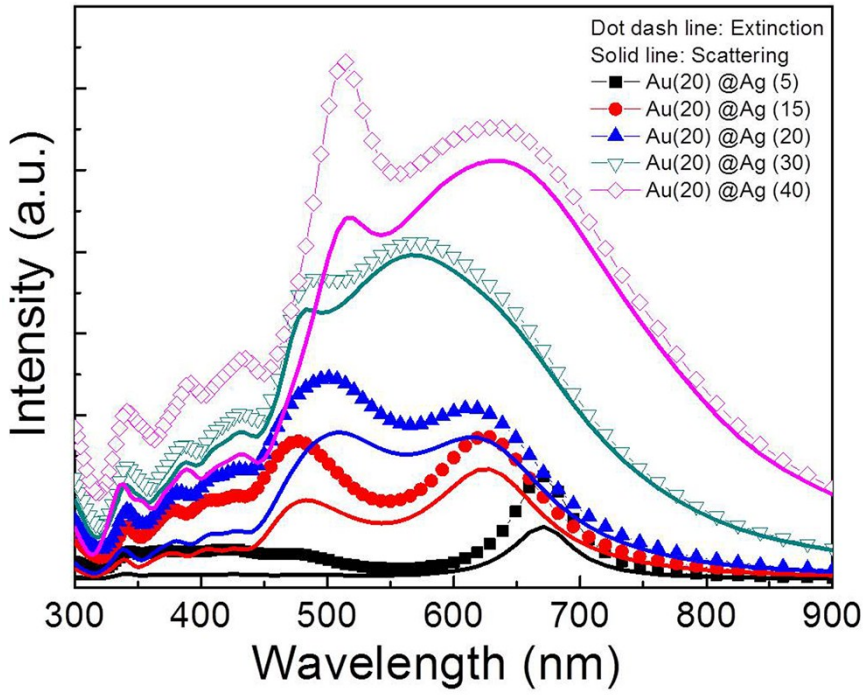


**Figure S6**. FDTD simulation of the extinction and scattering spectra for Au@Ag NCs with different Ag shell thickness (5, 15, 20, 30, 40 nm). Dot dash and solid line represent extinction and scattering curves, respectively.

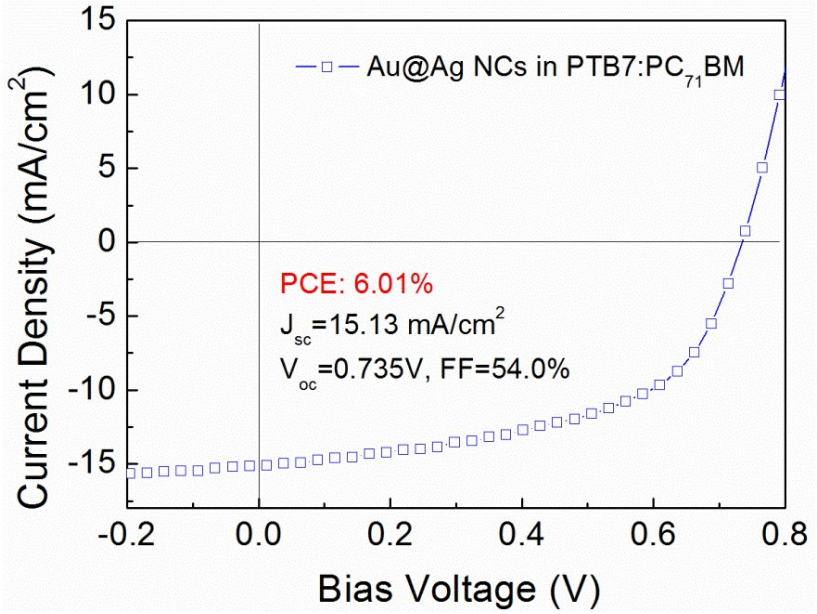


**Figure S7**. J-V characterization of the best OPV based on PTB7:$PC_{71}BM$ with Au@Ag NCs introduced in the active layer.

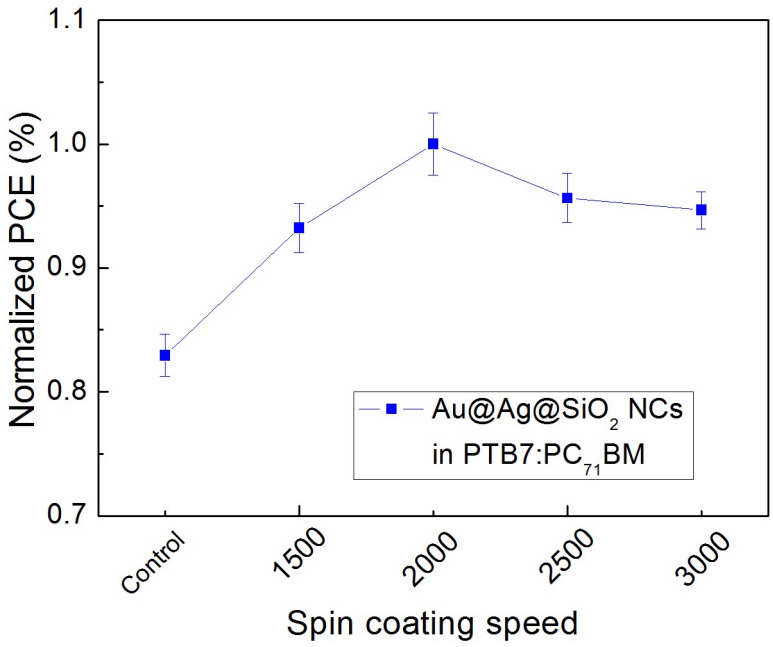


**Figure S8**. The normalized PCEs of the OPV devices based on PTB7:$PC_{71}BM$ with the addition of Au@Ag@$SiO_2$ in the active layer as a function of the spin coating speed. Control devices without Au@Ag@$SiO_2$ NCs were characterized as a reference.

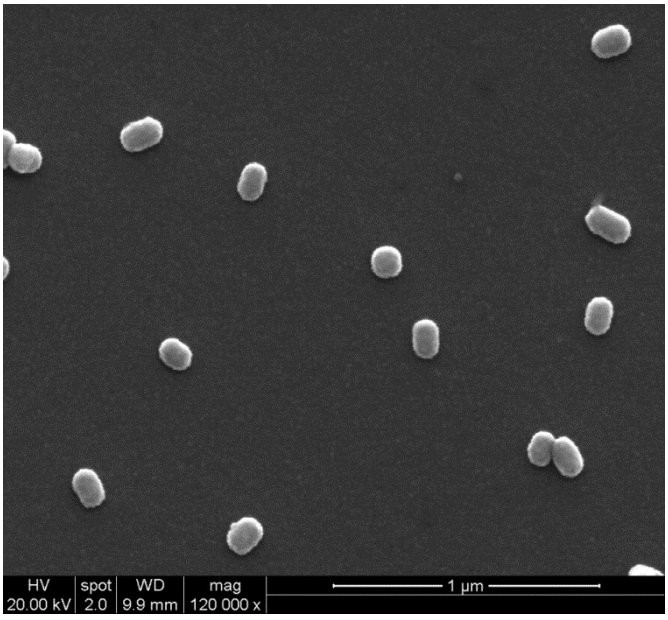


**Figure S9.** SEM image of well-distributed Au@Ag@$SiO_2$ NCs on PEDOT/glass substrate via spin coating with rotation of 2000 rpm for 30s.

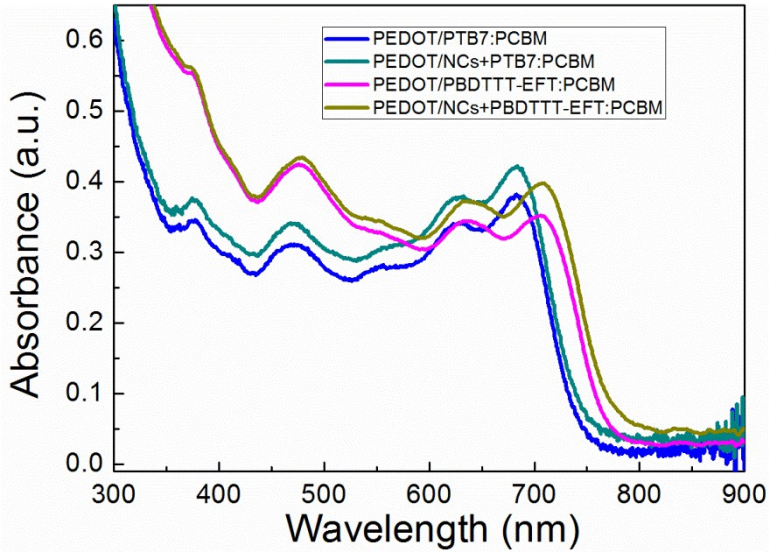


**Figure S10**. Light absorbance of the active layers (including PTB7:$PC_{71}BM$ and PBDTTT-EFT:$PC_{71}BM$) with or without Au(20nm)@Ag(20nm)@$SiO_2$(10nm) NCs embedded in them.

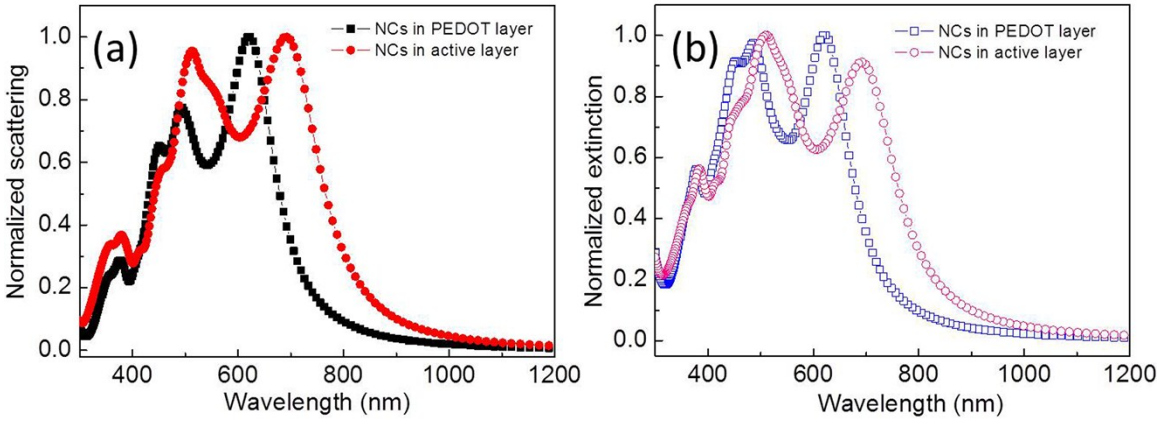


**Figure S11.** Simulated normalized (a) scattering and (b) extinction spectra for Au(20nm)@Ag(20nm)@$SiO_2$(10nm) NCs with different locations.

## Tables:

**Table S1**. Summary of photovoltaic performance of OPVs based on PTB7:$PC_{71}BM$ with different addition levels (solution volumn percentage) of Au(20 nm)@Ag(5 nm) NCs in PEDOT:PSS. (*Ag shell thickness is 5 nm*)

| Addition level of NCs in PEDOT:PSS | | $J_{sc}$ (mA/cm²) | $V_{oc}$ (V) | FF (%) | PCE (%) | Relative PCE Enhancement (%) |
|---|---|---|---|---|---|---|
| **Control** | Average | 16.64 | 0.738 | 64.5 | 7.92±0.21 | / |
| **1%** | Average | 17.26 | 0.742 | 64.8 | 8.30±0.17 | 4.8±2.1 |
| | Best | 17.54 | 0.748 | 64.7 | 8.49 | 7.2 |
| **5%** | Average | 17.07 | 0.751 | 66.0 | 8.46±0.19 | 6.8±2.4 |
| | Best | 17.17 | 0.751 | 67.1 | 8.65 | 9.2 |
| **10%** | Average | 17.27 | 0.747 | 64.8 | 8.36±0.08 | 5.6±1.0 |
| | Best | 17.77 | 0.747 | 63.9 | 8.48 | 7.1 |
| **20%** | Average | 16.70 | 0.750 | 66.6 | 8.34±0.09 | 5.3±1.1 |
| | Best | 16.90 | 0.750 | 66.5 | 8.43 | 6.4 |

**Table S2**. Summary of photovoltaic performance of OPVs based on PTB7:$PC_{71}BM$ with different addition levels (solution volumn percentage) of Au(20 nm)@Ag(15 nm) NCs in PEDOT:PSS. (*Ag shell thickness is 15 nm*)

| Addition level of NCs in PEDOT:PSS | | $J_{sc}$ (mA/cm²) | $V_{oc}$ (V) | FF (%) | PCE (%) | Relative PCE Enhancement (%) |
|---|---|---|---|---|---|---|
| **Control** | Average | 15.50 | 0.746 | 67.3 | 7.78±0.09 | / |
| **1%** | Average | 16.30 | 0.749 | 66.6 | 8.13±0.10 | 4.5±1.3 |
| | Best | 16.30 | 0.757 | 66.8 | 8.24 | 5.9 |
| **5%** | Average | 16.81 | 0.749 | 67.9 | 8.55±0.10 | 9.9±1.3 |
| | Best | 16.70 | 0.748 | 69.5 | 8.68 | 11.6 |
| **10%** | Average | 16.30 | 0.750 | 67.9 | 8.30±0.21 | 6.7±2.7 |
| | Best | 16.61 | 0.750 | 68.4 | 8.52 | 9.5 |
| **20%** | Average | 15.99 | 0.751 | 65.7 | 7.89±0.19 | 1.4±2.4 |
| | Best | 15.89 | 0.752 | 67.7 | 8.09 | 4.0 |

**Table S3**. Summary of photovoltaic performance of OPVs based on PTB7:$PC_{71}BM$ with different addition levels (solution volumn percentage) of Au(20 nm)@Ag(20 nm) NCs in PEDOT:PSS. (*Ag shell thickness is 20 nm*)

| Addition level of NCs in PEDOT:PSS | | $J_{sc}$ (mA/cm²) | $V_{oc}$ (V) | FF (%) | PCE (%) | Relative PCE Enhancement (%) |
|---|---|---|---|---|---|---|
| **Control** | Average | 16.64 | 0.738 | 64.5 | 7.92±0.21 | / |
| **1%** | Average | 17.11 | 0.743 | 65.6 | 8.34±0.18 | 5.3±2.3 |
| | Best | 17.83 | 0.745 | 64.3 | 8.54 | 7.8 |
| **5%** | Average | 18.01 | 0.749 | 65.6 | 8.85±0.17 | 11.7±2.2 |
| | Best | 18.91 | 0.745 | 64.3 | 9.06 | 14.4 |
| **10%** | Average | 17.79 | 0.746 | 65.4 | 8.68±0.06 | 9.6±0.6 |
| | Best | 18.26 | 0.748 | 64.0 | 8.74 | 10.4 |
| **20%** | Average | 17.16 | 0.747 | 64.5 | 8.27±0.18 | 4.4±2.3 |
| | Best | 17.36 | 0.747 | 65.3 | 8.47 | 6.9 |

**Table S4**. Summary of photovoltaic performance of OPVs based on PTB7:$PC_{71}BM$ with different addition levels (solution volumn percentage) of Au(20 nm)@Ag(30 nm) NCs in PEDOT:PSS. (*Ag shell thickness is 30 nm*)

| Addition level of NCs in PEDOT:PSS | | $J_{sc}$ (mA/cm²) | $V_{oc}$ (V) | FF (%) | PCE (%) | Relative PCE Enhancement (%) |
|---|---|---|---|---|---|---|
| **Control** | Average | 15.49 | 0.727 | 70.0 | 7.88±0.05 | / |
| **0.5%** | Average | 16.04 | 0.737 | 69.4 | 8.21±0.09 | 4.2±1.1 |
| | Best | 16.13 | 0.740 | 70.3 | 8.39 | 6.5 |
| **2.5%** | Average | 15.79 | 0.736 | 71.3 | 8.29±0.08 | 5.2±1.0 |
| | Best | 16.28 | 0.735 | 70.5 | 8.43 | 7.0 |
| **5%** | Average | 17.07 | 0.730 | 69.7 | 8.69±0.09 | 10.3±1.1 |
| | Best | 17.15 | 0.731 | 70.0 | 8.78 | 11.4 |
| **10%** | Average | 16.49 | 0.736 | 68.3 | 8.29±0.07 | 5.2±0.9 |
| | Best | 16.84 | 0.743 | 67.1 | 8.40 | 6.6 |

**Table S5**. Summary of photovoltaic performance of OPVs based on PTB7:$PC_{71}BM$ with different addition levels (solution volumn percentage) of Au(20 nm)@Ag(40 nm) NCs in PEDOT:PSS. (*Ag shell thickness is 40 nm*)

| Addition level of NCs in PEDOT:PSS | | $J_{sc}$ (mA/cm²) | $V_{oc}$ (V) | FF (%) | PCE (%) | Relative PCE Enhancement (%) |
|---|---|---|---|---|---|---|
| **Control** | Average | 15.49 | 0.727 | 70.0 | 7.88±0.05 | / |
| **0.5%** | Average | 15.40 | 0.731 | 70.5 | 7.94±0.09 | 0.8±1.1 |
| | Best | 15.47 | 0.731 | 71.6 | 8.10 | 2.8 |
| **2.5%** | Average | 15.89 | 0.735 | 69.2 | 8.08±0.14 | 2.5±1.8 |
| | Best | 15.89 | 0.739 | 70.4 | 8.27 | 4.9 |
| **5%** | Average | 16.01 | 0.731 | 70.8 | 8.29±0.07 | 5.2±0.9 |
| | Best | 16.00 | 0.731 | 71.6 | 8.37 | 6.2 |
| **10%** | Average | 15.46 | 0.728 | 70.1 | 7.89±0.01 | 0.1±0.1 |
| | Best | 15.39 | 0.728 | 70.6 | 7.91 | 0.4 |

**Table S6.** Incorporated metal nanoparticles and efficiencies of previously reported high-performance plasmonic OPVs with PCEs higher than 8%.

| Nanoparticle type | Active layer | Average PCE (%) | Relative PCE enhancement (%) | Year | reference |
|---|---|---|---|---|---|
| **Au@Ag nanocuboid** | PTB7:$PC_{71}BM$ | 9.48 | 22.8 | / | This work |
| **Au@Ag nanocuboid** | PBDTTT-EFT:$PC_{71}BM$ | 10.42 | 14.1 | / | |
| **Au NP +grating** | PBDTTT-C-T:$PC_{71}BM$ | 8.79 | 15.8 | 2012 | 33 |
| **Ag+Au nanosphere** | PTB7:$PC_{71}BM$ | 8.67 | 20.0 | 2013 | 25 |
| **Au nanocuboid** | PTB7:$PC_{71}BM$ | 8.52 | 17.5 | 2013 | 25 |
| **Carbon-dot-Ag NP** | PTB7:$PC_{71}BM$ | 8.31 | 10.4 | 2013 | 26 |
| **Ag@$SiO_2$ nanosphere** | PTB7:$PC_{71}BM$ | 8.49 | 16.9 | 2013 | 24 |
| **Ag NP** | PTB7:$PC_{71}BM$ | 8.60 | 8.9 | 2013 | 31 |
| **Au@Ag Nanocube** | PTB7:$PC_{71}BM$ | 8.74 | 12.3 | 2014 | 32 |
| **Au NP +grating** | PTB7:$PC_{71}BM$ | 9.34 | 22.1 | 2015 | 36 |